Bends in Polymeric Multimode Waveguides

Henry Kelderman, Mart B.J. Diemeer, Lucy T.H. Hilderink, and Alfred Driessen
University of Twente, Integrated Optical MicroSystems (IOMS) h.kelderman@ewi.utwente.nl

Abstract: *We developed photodefined, multimode-fiber compatible waveguides based on epoxies. The waveguides showed losses < 0.06 dB/cm at 832 nm and 633 nm. Propagation and bending losses are calculated and experimentally verified. The minimum allowable radius that can be connected to a straight waveguides are modeled and experimentally verified.*

Introduction

The continuous increase of the microprocessor clock-rate (expected clockfrequency $\sim 10^{10}$ Hz in 2011), in addition to the continuous increase of data rates in optical transmission systems, has created a bottleneck in high- end systems like servers, and telecom switches, at the interconnect between cards over their PCB (Printed Circuit Board) backplane. In those systems, aggregate data rates of multiple Tbps have to be transported via the backplanes over a typical distance of about 0.5 m. With such bandwidth-distance products, electrical data transmission through a copper line is touching its fundamental limit around 20 Gbps.
Optical transmission via waveguides offers the potential of a much larger capacity. Therefore, there is worldwide an intense research activity ongoing to realize Optical Backplanes. These are backplanes with an embedded multimode polymeric optical waveguide layer, equipped with in- and output couplers, fabricated with PCB compatible, low-cost fabrication techniques [1]. In [2] we reported on a photodefinable epoxy formulation with attractive properties for Optical Backplane applications. This paper shows propagation losses obtained from spiral structures and bending losses from U-shaped bends.

Waveguide Definition and Cross Section

The core of the waveguides presented in this paper is about $45 \times 45\ \mu m$. The core material used in the spirals was spun directly on the Pyrex substrate. This simplifies processing, but also introduces an asymmetry in the index below and surrounding the other sidewalls of the core. For the U-bends a bottom cladding was applied, resulting in a more symmetrical modal profile -as far as we can speak of modal profile in these highly multimodal waveguides- and subsequently a lower refractive index contrast can be used. Figure 1 shows a cross section of the several waveguides used in the U-bends.
For the U-bends the refractive index in the cladding is 1.514 and the core is 1.528 leading to an index contrast of 0.014. In the spirals a higher index contrast of 0.03 was used.

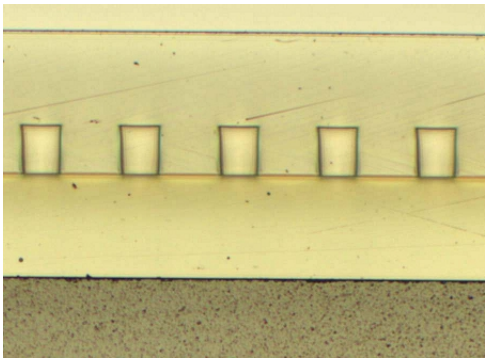

Fig. 1: Cross section of 5 waveguides used in U-bends.

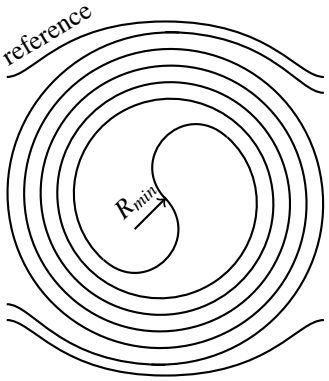

Fig. 2: Schematic layout of an Archimedean spiral with two reference waveguides.

Archimedean Spiral

Propagation losses in the order of 0.1 dB/cm are difficult to measure by cut-back measurements. Since differences in chiplength are typically centimeters, the differences in loss are in the same order as the fiber-chip coupling variation.
Therefore, we decided to create a waveguide of significantly longer length by curling it up in a spiral and comparing its losses to an on-chip shorter reference waveguide. The contribution of the bending loss will be limited when the curvature of the spiral and especially the S-bend in the middle is chosen appropriately i.e., the radius of curvature chosen large enough. The smallest radius will be found in the s-bend.
The mismatch of modes from connecting different curved waveguides e.g., in the center of the s-bend has been disregarded since improving it by adiabatically connecting different curvatures will result in a larger overall structure for which there was no space. The following section will show that this presumption did not introduce significant additional losses, which is a

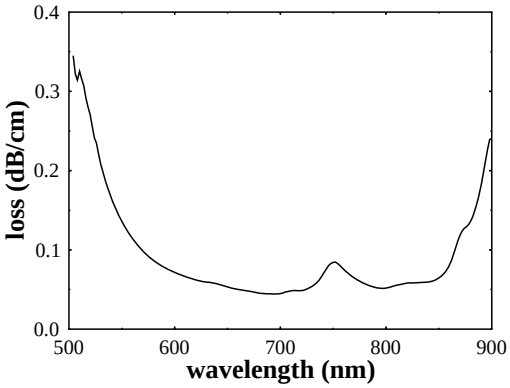

Fig. 3: Spectral dependence of propagation loss observed in spiral waveguide

result of the relatively high contrast used and the relatively large core dimensions.
An Archimedean spiral is defined by:

$$r = a\theta^{1/p} \tag{1}$$

We have set $a = 1.0$ and $p = 1.1$, and scaling appropriately to obtain more or less equidistant windings. The minimum radius used in the s-bend also defines the minimum radius in the spiral ($2R_{min}$). We have set R_{min} to $15mm$ leading to an approximate single winding length of $2 \times 2\pi R_{min} \sim 188mm$, where the pitch from winding to winding has been disregarded.
Equation 1 has been discretisized in θ leading to an array of points (r, θ). After transforming these to cartesian coordinates, these points have been connected by pieces of straight waveguides. Thus the curvature has been approximated by segmented lines. If the stepsize $\Delta\theta$ is chosen small enough this will be barely noticeable in the photomask.
The low contrast used ($NA = 0.2$) also allowed to use in-house laser beam written masks that typically have an edge roughness of ~150 nm. Propagation losses depicted here include scattering losses and an easy, albeit costly, improvement could be to use e-beam written photomasks.

Propagation Loss

To allow for accurate propagation loss measurements, a very long (103.6 cm) coiled up waveguide, combined with a short (7.2 cm) reference waveguide was made on a 4" Pyrex wafer. The long waveguide is an Archimedean spiral as shown in Figure 2.
Figure 3 shows the spectral dependance of the propagation loss in the spiral by subtracting the insertion loss for the reference waveguide and the spiral and accounting for the difference in propagation length.
To verify these losses we took a picture of a part of the spiral as shown in Figure 4. By integrating the intensity of the pixels over a small rectangle that captures just one waveguide, an estimate for the local power is

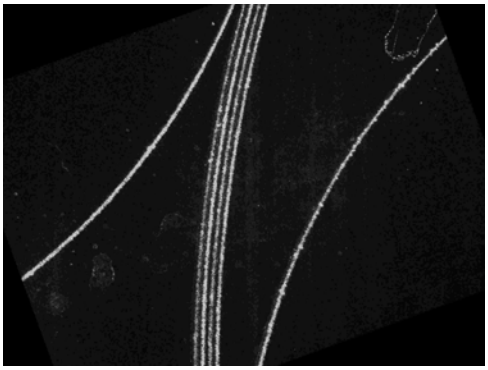

Fig. 4: Scattered light as observed from the top at 633 nm

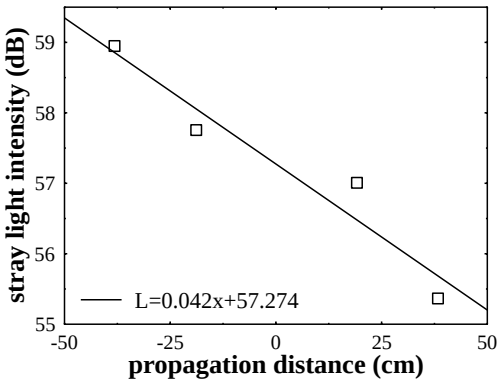

Fig. 5: Observed local intensity as function of propagated length in spiral.

obtained. This is done for the four waveguides that are close together and represent the four windings of the spiral. Since it is known how far the light propagated from one winding to the next, also accounting for the S-bend in the center, the intensity of each local area containing one waveguide can be set out versus its relative propagation length. Figure 5 shows the local scattered intensity versus the relative propagation length in the spiral, from that we can determine the propagation loss at 633 nm to be about 0.04 dB/cm. Which compares well to the values we found earlier.

Bend loss

The size of a spiral is determined by the radius of the arc used in the S-bend in the middle of the spiral where the losses are still acceptable. In order to find that 'cut-off' radius a sample has been made with varying radii. As depicted schematically in Figure 6 we choose a U-shaped bend where the total angle traveled is 360°. Note that the vertical section on the right hand side has been prolonged. This served two goals. Firstly it creates an offset between the input and the output. Secondly it was used to make the total propagation length in all U-bends exactly the same. Note that although in

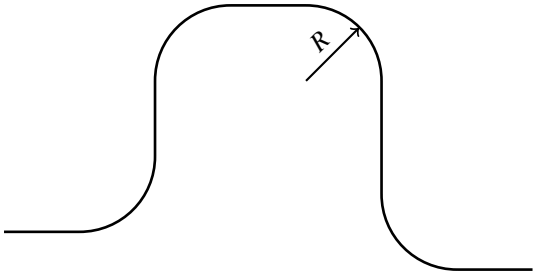

Fig. 6: Schematic 'U'-shaped bend

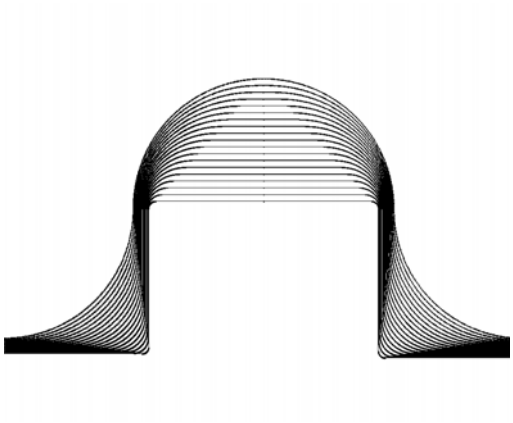

Fig. 7: Mask design showing multiple U-bends with varying radii.

Figure 6 only one U-bend has been shown, the radius has been varied from 1 to 19 mm in steps of 1 mm. See Figure 7 for resulting mask layout.

To determine the propagation loss, six straight reference waveguides have been placed on the same sample. The difference in length between U-bend and reference is 40 mm, which is expected to lead to an difference is loss of about 0.4 dB.

Figure 8 shows the insertion loss of the U-bends minus the loss found in the reference waveguide as function of the radius. Note that this introduces a systematic error of about 0.4 dB at wavelengths larger than 600 nm.

Reducing the bend radius gradually increases losses, until a certain cut-off is met, where losses increase rapidly. The transmission in the waveguides with the smallest radii seems to increase. This is an artifact that can be explained as follows; the light lost in the bend is not absorbed, and hence will find its way to the backside of the sample, leading to a background level of intensity. Especially in smaller radii where more light is lost, this effect is more predominant and makes alignment hard. The higher loss at 532 nm can partially be explained by the higher losses at that wavelength (cf. Figure 3).

The modeled response in Figure 8 can be calculated from [3]:

$$L = 10 \cdot^{10} \log\left(1 - \frac{t}{2R} - \frac{t^2}{2R^2} - \frac{t^3}{2R^3} - \frac{t^4}{2R^4}\right) \quad (2)$$

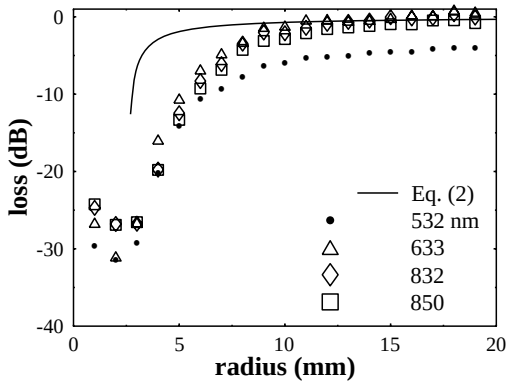

Fig. 8: Observed losses in 'U'-shaped bends at four different wavelengths.

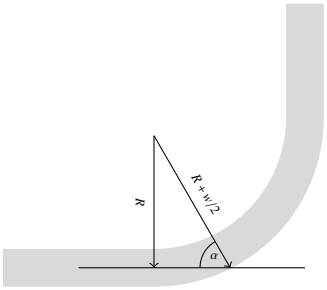

Fig. 9: A ray traveling in the middle of the waveguide coming from the right, would strike the normal to the tangent of the outer perimeter of the bend at an angle α.

where $t = (n_{core}^2 w)/(NA)^2$, w is the width of the waveguide and NA is the Numerical Aperture. The model fails when $t/R < 0.5$, but adequately describes the experimental results as shown in [4]. The offset in the cut-off region in our experimental data can be explained by the fact that in the U-bend eight straight-bend coupling areas are introduced, and the model includes only the effects of a circular bend.

Further inspection revealed that light is escaping the bend predominantly in the first part of the curved section, and not continuously over the entire bend as might have been suspected.

This can partially be explained by the angle at which a ray strikes the outer perimeter of the bend as shown in Figure 9. Suppose we were to look at a ray traveling in the middle of the straight waveguide. It would strike the outer perimeter at an angle α to the normal of the tangent described by:

$$\alpha = \arcsin\left(\frac{R}{R + w/2}\right) \quad (3)$$

If we use this angle in the Fresnel equation for s-

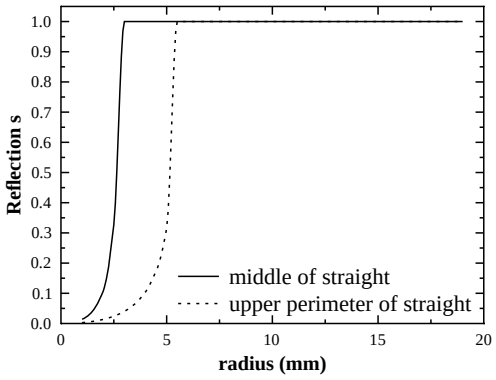

Fig. 10: Reflection coefficient from a ray travelling in the middle of the straight waveguide striking the outer perimeter of the curved section as function of the radius. Also shown is the reflection of a ray traveling along the upper boundary of the straight waveguide.

polarisation:

$$R_s = \frac{n_{core}\sin\alpha - n_{cladding}\sin\theta_2}{n_{core}\sin\alpha - n_{cladding}\sin\theta_2} \qquad (4)$$

where θ_2 can be obtained from Snell's law of refraction. we obtain Figure 10. Although not shown here, p-polarisation will result in almost the same fraction of light reflected. Without taking into account that the actual angles of the rays will vary, this simple description accurately estimates the minimum radius that can be connected without loss to a straight waveguide.
This argument does not directly explain the non-continuous loss through the bend. If we were to consider a ray traveling along the tangent of the inner perimeter of the bend, which is the ray that has the smallest angle to the normal and hence experience the lowest reflection. This specific ray would have been reflected at an earlier point in the bend at the same angle, therefore its power would have been reduced significantly upon the first reflection, provided the angle is sufficiently small.

Conclusion

We have presented multimode photodefinable waveguides for Optical Backplane applications. A propagation loss of <0.06 dB/cm at 850 and 633 nm has been measured in spirals using two methods; 1) from the difference in length and the obtained insertion loss thereof and 2) from analysis of the scattered light of different locations in the spiral. For a refractive index contrast of 0.014 (NA=0.2) we experimentally found that the minimum usable radius is 10 mm and verified this by simple calculation of Fresnel reflection and also compared this to a model by Israel et al. It has been shown that within the wavelength region measured (530-850 nm) the loss in bends as function of radius is independent of wavelength.

Acknowledgments

The authors acknowledge the financial support of Dutch Foundation STW (project TOE 6986) and wish to thank Anton J.F. Hollink for his support.

References

[1] C. Berger, R. Beyeler, G.-L. Bona, R. Dangel, L. Dellmann, P. Dill, F. Horst, M. Kossel, C. Menolfi, T. Morf, B. J. Offrein, M. L. Schmatz, T. Toifl, and J. Weiss, "Optical links for printed circuit boards," in 16th Ann. Meeting of IEEE Lasers & Electro-Optics Soc., October 26-30, Tucson, AZ, USA, 2003.

[2] Mart Diemeer, Lucie Hilderink, Ronald Dekker and Alfred Driessen, "Low-cost and low-loss multimode waveguides of photodefinable epoxy", IEEE Photon. Technol. Lett., vol. 18, no. 15, pp. 1624-1626, 2006.

[3] D. Israel, R. Baets, N. Shaw, and M.J. Goodwin, Techn. Digest MOC/GRIN, 1993.

[4] Sami Musa, Albert Borreman, A.A.M Kok, M.B.J. Diemeer, and Alfred Driessen, "Experimental study of multimode optical waveguides", Appl. Optics, vol. 43 no. 40, October 2004.